JOURNAL OF SOLID STATE CHEMISTRY 45, 180–192 (1982)

Raman Spectra and Valence Force Field of Single-Crystalline β Ga_2O_3

D. DOHY AND G. LUCAZEAU

Laboratoire de Chimie–Physique, Université Paris XIII, Avenue J. B. Clément, 93430 Villetaneuse, France

AND A. REVCOLEVSCHI

Laboratoire de Chimie Appliquée, Université Paris-Sud, 91405 Orsay Cedex, France

Received February 5, 1982

Single-crystalline β Ga_2O_3 was studied by Raman spectroscopy between 10 and 1000K. A complete valence force field was obtained. The agreement between observed and calculated Raman active frequencies is 0.8% for the whole spectrum. The potential energy distribution shows that stretching and bending modes are not independent. A complete description of the modes is given in terms of cartesian displacements. The temperature dependence of the Raman band half-widths was studied and is discussed in terms of anharmonicity at high temperature; the broadening which appears above 100K seems to be related to the appearance of defects. Our spectra are better understood in terms of the $C2/m$ space group proposed by Geller rather than $P1$ as recently proposed by G. M. Wolten and A. B. Chase (*J. Solid State Chem.* **16**, 377, 1976).

I. Introduction

This work was undertaken as part of a general study of oxides, in particular those belonging to the β alumina family. Like that of β aluminates (11 Al_2O_3–M_2O) and β gallates, the structure of β Ga_2O_3 is made of GaO_6 (edge sharing) octahedra and GaO_4 (corner sharing) tetrahedra. Preliminary Raman results (*1a*) have shown that the β Ga_2O_3 spectra are much simpler than those of stoichiometric β gallates, due to the fact that the unit cell multiplicity is much lower in the former. In these conditions it seemed interesting to undertake a complete infrared and Raman study of a single crystal of β Ga_2O_3 in order to deduce a reliable valence force field transferable to β Al_2O_3 allowing the interpretation of the spectra of this compound (*1b*, *2*). The structure of β Ga_2O_3 reported by Geller (*3*) has been criticized recently by Wolten and Chase (*4*). Therefore it seemed of interest to look for structural information from spectroscopy experiments. There are only a few spectroscopic data (*5*) which are of no use for the assignment of the different bands either in terms of symmetry or in terms of internal coordinates.

Moreover, although no first-order phase transition has been detected by DTA in the 200 to 500-K temperature range (*6a*) it seemed interesting to investigate the role played by the anharmonicity and also the

0022-4596/82/140180-13$02.00/0

existence of possible phase transitions in the 10- to 1000-K range. These phenomena are usually detected from the temperature dependence of frequencies and half-widths of Raman and ir bands.

Finally, this work was undertaken as the first step of a study of a series of Ga_2O_3 crystals doped with ions such as Cr^{3+}, having possible lasing properties. Preliminary Raman results (*6b*) corroborate ESR results (*3*), i.e., for concentrations as high as 3% Cr^{3+}, the crystal structure remains ordered, indicating that Cr^{3+} substitutes Ga^{3+} ions.

II. Experimental

1. Crystal growth. β Ga_2O_3 was prepared by heating 99.9999% gallium hydroxide GaO(OH) in air at 1000°C for 12 hr. Single crystals were grown by a floating zone method (*6c*), associated with an image furnace in which the light source consists of a 6.5-kW xenon lamp.

A crystal was cut and oriented following indicatrix axes. A parallepiped of 4 × 2 × 1 mm was obtained for which the C_2 axis (*b* axis) was taken as the *Z* axis (Fig. 1). The axis direction was verified through Laüe patterns (a polarizing microscope observation was not sufficient). The *Y* axis coincides with the *a* crystallographic direction: it is parallel to the n_m axis of the indices ellipsoid. The *X* axis was taken orthogonal to the *Y* and *Z* axes; it defines an angle of 13.7° with the *c* axis in the (*ac*) plane.

2. Spectra. Polarized Raman spectra of the single-crystalline sample were recorded on a Coderg T 800 instrument equipped with an ionized argon laser. The polarizations reported in Fig. 4 and Table I are based on the Porto's notation. Leaks into unallowed polarization are less than 2%. Low-temperature spectra (10–300K) were obtained by immersing the crystal in 4-K gaseous helium, the temperature being controlled by thermocouple. At high temperature (300–1000K) four independent series of measurements were performed in order to obtain precise curves representing the half-width variations as a function of temperature. Measurements were carried out every 25K between 4 and 673K for the most sensitive modes. The curve corresponding to the 353-cm^{-1} mode is not reported, because the 345-cm^{-1} mode overlaps this band and the deconvolution is not reliable for large half-widths.

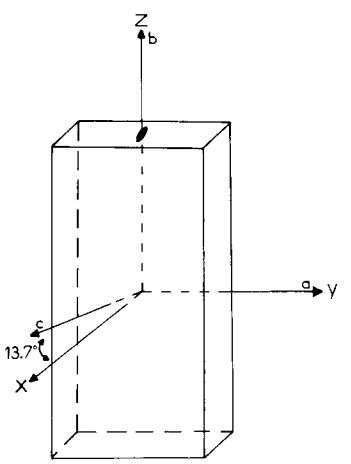

FIG. 1. Relation between crystallographic *a,b,c* axes and observed *X, Y, Z* axes for the β Ga_2O_3 single crystal (4 × 2 × 1 mm) used in this study.

III. Structure and Selection Rules

According to Geller, β Ga_2O_3 has a monoclinic structure and belongs to the C_{2h}^3 space group; the unit cell contains two formula units (Fig. 2b). There are two crystallographically nonequivalent gallium and three nonequivalent oxygen ions in the unit cell. Each Ga_I^{3+} ion is surrounded by a distorted tetrahedron of oxygen ions: one O_I^{2-} ion at 1.80 Å, two O_{II}^{2-} ions at 1.83 Å, and one O_{III}^{2-} at 1.85 Å. Each Ga_{II}^{3+} ion is surrounded by a distorted octahedron of oxygen: two O_I^{2-} at 1.95 Å, one O_{II}^{2-} at 1.95 Å, two O_{III}^{2-} at 2.08 Å, and one O_{III}^{2-} at 2.02 Å. A tetrahedron shares only corners with other tetrahedra in the *b* axis direction and with

TABLE I

INFRARED AND RAMAN SPECTRA OF β Ga_2O_3 AT DIFFERENT TEMPERATURES

Infrared[a] (K)		Raman (K)			Polarization relative intensities[b]					
100	300	10	300	800	XX	YY	ZZ	XY	YZ	XZ
			111	108	45	—	*	—	—	*
		115	114	112	—	—	—	—	10	20
		147	147	140	*	—	—	*	70	45
		170	169	165	135	65	55	—	*	*
	155 m	200	199	199	1000	175	315	15	5	15
	250 m									
	275 m									
	290 m									
	310 sh									
		319	318	317	45	20	20	25	*	*
		347	346	340	20	185	120	*	*	*
		355	353		—	—	—	—	15	*
375 S	375 m									
		415	415	414	125	175	110	35	*	*
455 S	455 S									
		475	475	468	75	*	60	*	*	40
525 sh	525 sh									
		629	628	620	115	*	25	10	*	*
640 sh	640 sh									
		651	651	640	—	—	—	—	10	110
		657	657	648	*	125	*	70	—	—
668 S	668 F									
720 sh	720 sh									
760 m	760 m									
		767	763	754	65	595	—	25	*	*

[a] S: strong; m: mean, sh: shoulder.

[b] Raman spectra of a single crystal at 300K: relative intensities for different polarizations. XX, YY, ZZ, XY are the elements of scattering matrices corresponding to A_g modes, YZ and XZ are relative to B_g modes; an intensity of 1000 has been given to the XX component of the 199-cm^{-1} band.

* Indicates bands of low intensity probably due to polarization leaks into unallowed components (<2%).

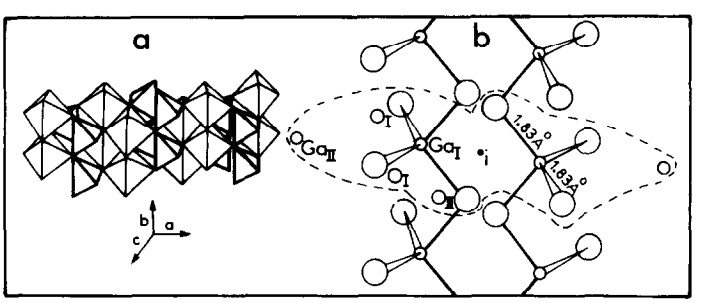

FIG. 2. (a) Representation of the tetrahedra and octahedra which form the structure of β Ga_2O_3. (b) Schematic representation of the unit cell of β Ga_2O_3; the atoms which are considered to define the $k = 0$ motions are included inside the broken line.

octahedra in other directions (Fig. 2a). An octahedron shares edges with adjacent octahedra. Each O_I^{2-} ion is at the corner of two octahedra and one tetrahedron; each O_{II}^{2-} is at the corner of one octahedron and two tetrahedra. Each O_{III}^{2-} ion is at the corner of three octahedra and one tetrahedron.

This structure has been criticized by Wolten and Chase. These authors claim that β Ga_2O_3 crystals are twinned and that they belong to the triclinic system and that their structure is described by the noncentrosymmetric space group C_1^1 with two formula units per cell.

Under the C_{2h} factor group the $k = 0$ crystal modes can be classified according to

$$\Gamma = 10\,A_g + 5\,B_g + 10\,B_u + 5\,A_u$$

from which acoustic modes $(A_u + 2\,B_u)$ must be substracted. Therefore 15 Raman and 12 infrared active modes are expected. Under the C_1 factor group one expects 27 modes both infrared and Raman active.

When only the shortest Ga–O bonds are considered, one can define the structure as made of chains of GaO_4 tetrahedra between which one finds "isolated" Ga_{II} ions. Furthermore, one can discriminate between $Ga_I(O_I)_2$ groups of atoms located in (010) planes and $Ga_I(O_{II})_2$ groups constituting chain links (Fig. 2b).

This approximate description is useful to describe the normal modes of the crystal; moreover, it is consistent with the fact that force constants decrease when the bond lengths increase, i.e., long bonds do not contribute at a large extent to the vibrational energy. For each Ga_IO_4 group of C_s site symmetry, one expects three stretching modes: on the one hand there are ν_s GaO_2 of A' symmetry and ν_a GaO_2 of A' symmetry which describe the in-plane symmetric and antisymmetric stretching modes of the $Ga_I(O_I)_2$ groups, respectively; on the other hand there is the ν $Ga_I(O_{II})_2$ mode describing the stretching of the bonds belonging to the chains. For $k = 0$ only one stretching mode remains because of the fact that the two oxygen atoms connected to a given Ga_I ion are congruent. In the same way bending modes can be defined for the tetrahedra. These are reported in Table II and Fig. 3 gives a description of these above-discussed vibrations. Motions of oxygen atoms common to tetrahedra and octahedra are considered deliberately as belonging to tetrahedra vibrations, therefore the pure octahedra vibrations are generated by the Ga_{II} translations. Thus 22 internal modes are described. Finally, by considering the R'_y librations of chains around the b axis and the three translations of each chain, one obtains eight external modes.

IV. Results and Discussion

1. Qualitative Assignments of Spectra

By considering Fig. 4 one can find ten bands in the XX polarization and five bands for the XZ spectrum. These bands appear at different frequencies with the exception of the 475-cm^{-1} band which is observed in

TABLE II

SYMMETRY CORRELATION FOR LOCALIZED COORDINATES

Number	Localized coordinates		Site group C_s	Space group C_{2h}
1	ν_s $Ga_I(O_I)_2$		A'	$A_g + B_u$
2	δ $Ga_I(O_{II})_2$		A'	$A_g + B_u$
3	ν_a $Ga_I(O_{II})_2$		A''	$A_u + B_g$
4	ν_a $Ga_I(O_I)_2$		A'	$A_g + B_u$
5	δ $Ga_I(O_I)_2$		A'	$A_g + B_u$
6	Rock.$_\perp$ $Ga_I(O_I)_2$		A''	$A_u + B_g$
7	Rock.$_\parallel$ $Ga_I(O_I)_2$		A'	$A_g + B_u$
8	Twist. $Ga_I(O_I)_2$		A''	$A_u + B_g$
9	Translations of	T_x	A'	$A_g + B_u$
10	Ga_{II}	T_y	A''	$A_u + B_g$
11	(octahedron modes)	T_z	A'	$A_g + B_u$
12	Libration of chains	R'_y	A'	$A_g + B_u$
13	Translations	T'_x	A'	$A_g + B_u^a$
14	of	T'_y	A''	$A_u^a + B_g$
15	chains	T'_z	A'	$A_g + B_u^a$

Note. These coordinates are defined in Fig. 3 and used in the description of normal modes reported in Table IV.

[a] Acoustic modes.

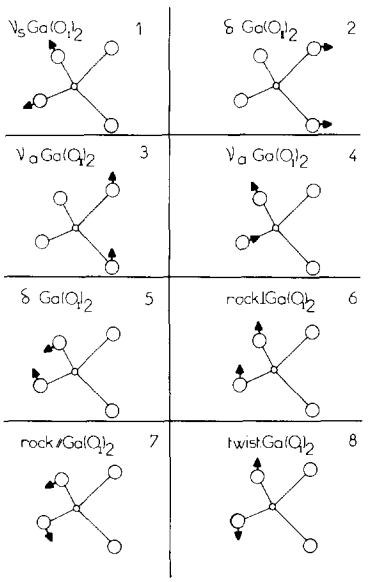

FIG. 3. Localized vibrations (chemically significant).

both (A_g and B_g) symmetry classes. It is interesting to note that polarization measurements allow the separation of the 111- to 114- and 345- to 353-cm^{-1} components. In other words, the 10 A_g + 5 B_g modes expected for the C_{2h} factor group are observed. This is confirmed by the low-temperature Raman spectrum (the crystal was misoriented on purpose) which contains 11 strong bands and two shoulders at about 350 and 660 cm^{-1}, respectively. Moreover, infrared and Raman exclusion can be checked on Fig. 5. It is possible to count 11 infrared maxima (the very weak bond at 275 cm^{-1} is probably due to an overtone) assignable to the 12 expected infrared active modes. These observations agree with the C_{2h} centrosymmetric structure proposed by Geller (*3*) rather than with the C_1 factor group proposed recently by Wolten and Chase (*4*). Table I reports the relative intensities for the different polarizations for each Raman band along with the infrared frequencies. Their assignment in terms of symmetry is reported unambiguously for Raman active modes.

A qualitative assignment can be proposed in order to define spectral regions in which it is reasonable to expect characteristic motions of the crystal before performing any calculations. In this respect three regions can be identified in the Raman spectra. The first region below 200 cm^{-1} is well separated from the high-frequency region by a gap of 100 cm^{-1}. This region is characterized by narrow bands ($\simeq$3 cm^{-1} at 300K) as compared to the other modes (7 cm^{-1}). These

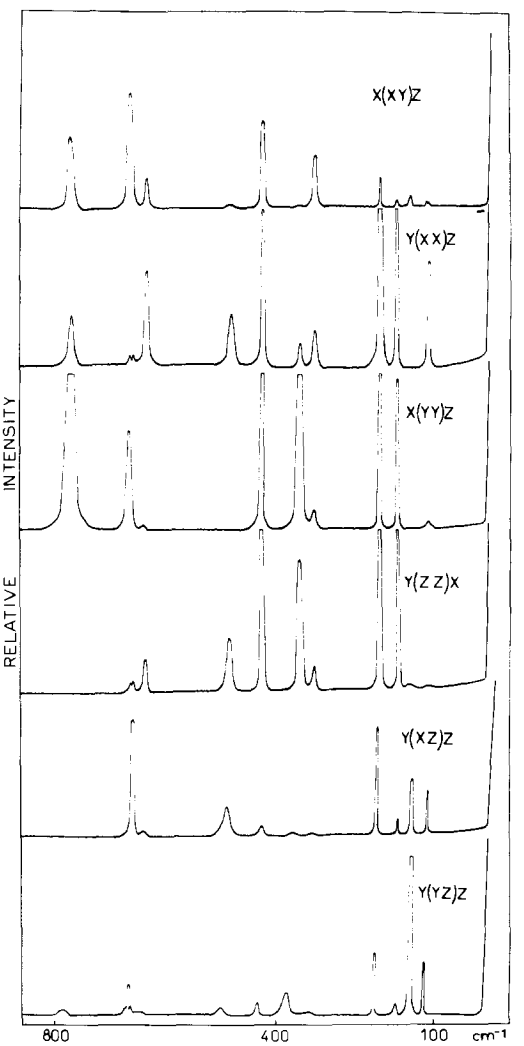

FIG. 4. Polarized Raman spectra of a single crystal of β Ga_2O_3 at 300K.

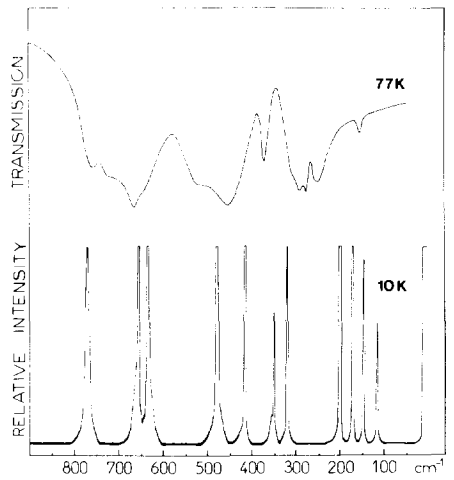

FIG. 5. Infrared and Raman spectra of polycrystalline β Ga_2O_3 at low temperature.

bands must be related to lattice modes corresponding to motions of small amplitude, such as vibrations involving the tetrahedra chains as a whole (translation and libration motions). The frequencies above 200 cm^{-1} should belong to vibrations which can be considered as internal vibrations, i.e., bending and stretching modes of tetrahedra groups. Considering the chemical description reported in the structural part of this article and the approximation of localized vibration coordinates (Fig. 3 and Table II), one can expect that stretching modes of tetrahedra occur at high frequency; in particular it seems reasonable to assign the highest frequency observed at 763 cm^{-1} to a stretching mode involving $Ga-O_I$ bonds, which are the shortest ones. The bending modes of tetrahedra are expected in the range 400–600 cm^{-1}, while vibrations involving motions of octahedra (translations of Ga_{II}) take place probably below 400 cm^{-1}.

2. *Valence Force Field Calculations*

Calculations were performed with a program of Shimanouchi's type (*7*). The force constants matrix was set up by using weighted symmetrical cartesian coordinates.

In the calculation 50 atoms were taken into account: those of the unit cell and their closest neighbors. Cartesian coordinates were deduced from the X-ray data reported by Geller (*3*). Two oxygen atom families and two types of gallium atoms were considered to define internal coordinates. The 11 internal coordinates are divided into four GaO stretching coordinates (f_{t1}, f_{t2}, f_{o1}, f_{o2}), six bending coordinates ($f\delta_1$, $f\delta_2$, $f\theta_1$, $f\theta_2$, $f\theta_3$, $f\gamma$), and a torsional coordinate τ (around the Ga–O bonds). These coordinates are represented in Fig. 6.

We considered 29 distinct force constants (11 diagonal and 18 interaction force constants). For every normal mode, cartesian displacements (LX) and potential energy distribution (PED) were calculated. Several force constants sets were tested; in particular, we tried a linear dependence of the four valence force constants as a function of the Ga–O distance. A refinement using least-squares method was performed; however, the correlation matrices have shown that force constants related to internal coordinates of octahedra were strongly dependent on those characteristic of tetrahedra (for example, force constants 1–5 were correlated with a factor of −0.62). Finally, the best agreement between experiments and calculations was obtained by letting valence force constants vary freely. In these conditions we observed a linear relationship $\nu = f(d)$ for two stretching constants of octahedra and one of tetrahedra. The second tetrahedra force constant is lower than what could be expected from this relationship (Fig. 7). Table III gives the final values for force constants. The atoms involved in the associated internal coordinates are also reported. A remarkable agreement between calculated and observed Raman frequencies is obtained. The error on the whole spectrum is less than 0.8%. On the other

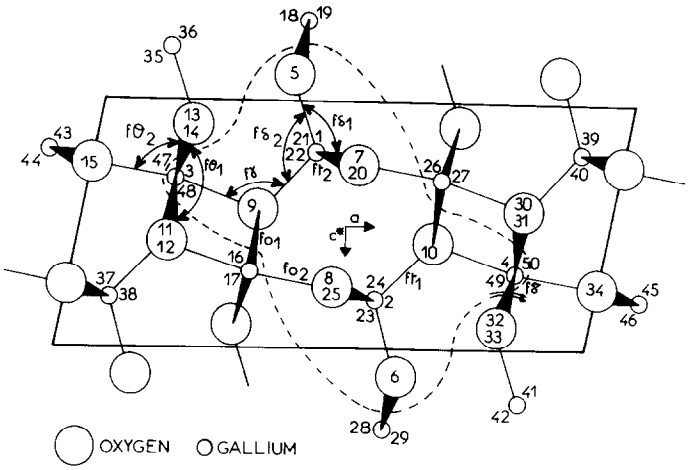

FIG. 6. Definition of internal coordinates used in the valence force field calculation. The primitive cell is inside the broken line.

hand, the agreement between infrared frequencies and A_u, B_u calculated frequencies is not so good, except for the narrow bands measured at 155 and 372 cm^{-1}. This disagreement is not surprising when one realizes that the infrared spectrum was recorded on a polycrystalline sample dispersed in nujol. The infrared bands corresponding to strongly polar modes lie between TO and LO frequencies (in between is the Reststrahlen region); therefore the observed maxima cannot coincide with the calculated frequencies. We can notice that the transverse mode for which the macroscopic electric field is weak must lie nearby the calculated frequency.

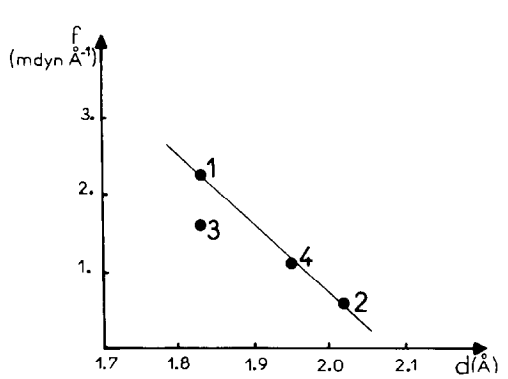

FIG. 7. Relationship between the stretching force constants and the bond length for Ga–O bonds: $f(\text{mdyne Å}^{-1}) = -8.628d\ (\text{Å}) + 18.05$.

Moreover, we confirm that the Raman band at 475 cm^{-1} is a superposition of two modes of A_g and B_g symmetry, the corresponding calculated frequencies being 474 and 468 cm^{-1}, respectively.

Two types of stretching force constants are found. The first one concerns the Ga–O bonds located in the (010) mirror plane and those of the (001) plane containing the axes of tetrahedra chains. They represent the strong bonds of the crystal. The second type corresponds to Ga–O bonds belonging to the square plane of the octahedron (defined by atom numbers 11, 12, 13, and 14 in Fig. 6) and is weaker (0.6 mdyne $Å^{-1}$) than the preceding one. The (100) and (001) planes are two cleavage planes in β Ga_2O_3 (*6c*). The results obtained from this valence force calculation show that the most probable cleavage planes are those which do not intersect chains axes, i.e., the (100) and (001) planes. Moreover, the (001) plane seems to be the easiest plane for cleavage. This can be seen from the following considerations. The potential associated with a definite bond can be described by a Morse function $V_n = D_e\ (1 - e^{-\beta x})^2$. The force

TABLE III

DEFINITION OF FORCE CONSTANTS

Number	Force constants	Calculated values (mdyne Å^{-1})	Examples of atoms involved in the corresponding internal coordinate
		Stretching	
1	f_{t_1}	2.25	Ga_1-O_5
2	f_{o_1}	0.60	Ga_3-O_{13}
3	f_{t_2}	1.62	Ga_1-O_7
4	f_{o_2}	1.27	Ga_3-O_9
		Bending	
5	$f\theta_1$	0.45	$O_{13}-Ga_3-O_{11}$
6	$f\theta_2$	0.45	$O_{11}-Ga_3-O_9$
7	$f\delta_1$	0.50	$O_5-Ga_1-O_7$
8	$f\delta_2$	0.61	$O_5-Ga_1-O_9$
9	$f\theta_3$	0.36	$O_{11}-Ga_1-O_{14}$
10	f_γ	0.5	$Ga_1-O_9-Ga_3$
		Torsion	
11	$f\tau$	0.02	Torsion around Ga_1-O_7 axis
		Stretching–stretching interactions	
12	$f_{t_1o_2}$	0.08	
13	$f_{t_1t_1}$	0.30	
14	$f_{t_1t_2}$	0.25	
15	$f_{o_1o_1}$	0.08	
16	$f_{o_1o_2}$	−0.03	
17	$f_{o_1o_2}$	−0.14	
18	$f_{o_2o_2}$	−0.08	
		Bending–bending interactions	
19	$f\theta_1\theta_2$	0.35	
20	$f\theta_2\theta_2$	0.05	
21	$f\theta_2\gamma$	0.19	
22	$f\theta_2\delta_1$	−0.1	
23	$f\theta_2\delta_2$	0.1	
24	$f\delta_1\delta_2$	−0.2	
25	$f\delta_1\gamma$	0.15	
26	$f\gamma\gamma$	−0.06	
		Stretching–bending interactions	
27	$f_{t_1}\delta_1$	0.26	
28	$f_{o_2}\theta_1$	−0.36	
29	$f_{t_T} = f_{o_T}$	0.35	

constant is the second derivative of V_n and is equal to $2\ \beta^2 D_e$; therefore the force constant is proportional to the dissociation energy D_e. Thus, when one considers the breaking of 9–16 and 27–10 bonds (Fig. 6), i.e., when one performs a cleavage following the (001) plane, one will have to spend a dissociation energy equal to twice $D_{(001)} = 0.6/2\beta^2$ (where 0.6 is the valence force constant for this bond); on the other hand, if such a cleavage is imagined occurring along the (100) plane the dissociation energy would be twice $D_{(100)} = 1.3/2\beta^2$. Therefore one realizes that the (001) plane is an easier cleavage plane than the (001) plane.

The potential energy distribution for each mode has been obtained. Table IV reports contributions to the potential energy originating from principal force constants larger than or equal to 15%. It is difficult to give a description of vibrations from the PED reported in this table, since the vibrations seem to be heavily mixed and, moreover, the internal coordinates are unappropriate to give a chemical description of vibrations; this is due to the fact that the valence force field used here does not take into account the local symmetry. In particular, atoms are distributed into layers; each atom is in a symmetry plane and therefore it should be more interesting to consider localized internal coordinates of the type of those reported in Table II.

Table IV gives a description of normal modes in terms of the localized coordinates introduced in Table II and Fig. 3. For instance, for the frequency calculated at 760 cm^{-1} the displacements of atoms involve motions corresponding to localized coordinates 1 and 5 (Fig. 3). As an example, four normal coordinates are represented in Fig. 8 and were chosen to cover the whole frequency range. One corresponds to a vibration which is mainly a pure asymmetric stretching mode of the $Ga_I(O_I)_2$ group of atoms. It is calculated at 628 cm^{-1}. The mode at 360 cm^{-1} corresponds to oxygen displacements perpendicular to the (010) plane and can be assigned to a twisting of the $Ga_I(O_I)_2$ group. It is worth noting that for these two normal coordinates, the gallium displacements are nearly equal to zero. On the other hand, for the modes at 195 and 113 cm^{-1}, the gallium atom displacements are strongly involved. The 113-cm^{-1} mode

TABLE IV

NORMAL MODES OF β Ga_2O_3

Frequency			Assignments of the modes			
Obs.						
Raman	ir[a]	Cal.	Symmetry	PED[b]	LX[c]	Description
763		760	A_g	$24f_t + 20f_o$	1 + 2	Stretching and bending of Ga_tO_4
	760	731	B_u	$17f_t + 29f_o$		
	720	692	B_u	$22f_o$		
	668	656	A_u	$62f_t + 16\delta_1$		
657		654	A_g	$41f_t + 22f_o + 15\delta_1$	2 + 5	
651		644	B_g	$65f_t + 17\delta_1$	3	
	640	626	B_u	$64f_t + 16f_o$		
628		628	A_g	$75f_t$	4	
	525	526	B_u	$91f_t + 20\delta_1 + 18\delta_2$		
475		474	A_g	$34f_t + 36f_o + 20\delta_1 + 16\delta_2$	1 + 5	
475		468	B_g	$39f_o + 30\delta_1 + 17\delta_2$	6	Deformation of $Ga_t(O_1)_2$ Octahedron modes
	455	500	A_u	$34f_o + 29\delta_1 + 15\delta_2$		
415		406	A_g	$33f_o + 18\delta_2$	7 + 9	
	375	374	B_u	$33\delta_3$		
353		360	B_g	$59f_o + 32\delta_1 + 16\delta_3$	8	
	n.o.	352	A_u	$16f_t + 64f_o + 25\delta_3$		
346		353	A_g	$22f_o + 39\delta_3$	9 + 7	
318		308	A_g	$20f_t + 32f_o + 21\delta_2$	11	
	310	337	B_u	$17f_t + 24f_o + 19\delta_2$		
	290	300	B_u	$16f_t + 30f_o + 15\delta_1$		
	250	216	A_u	$38\delta_1 + 21\delta_2 + 20\delta_3$		
199		195	A_g	$29f_o + 32\delta_1$	12	Libration and translations of chains
169		166	A_g	$15f_t + 39\delta_1 + 27\delta_2 + 33\delta_3$	13	
	155	155	B_u	$26f_t + 52f_o + 71\delta_1$		
147		152	B_g	$33f_t + 21\delta_1 + 16\delta_2 + 23\delta_3$	14	
114		114	B_g	$31f_o + 81\delta_1 + 98\delta_2$	10	
111		113	A_g	$62\delta_1 + 64\delta_2$	15	

[a] Infrared maxima measured by transmission; for broad and strong ir bands, the frequency of the maxima lies between TO and LO frequencies, the calculated corresponding frequency is probably rather near the TO component.

[b] f_t = Tetrahedron stretching; f_o = octahedron stretching; δ_1 = Ga–O–Ga bending; δ_2 = Ga_{II}–O_2 bending; δ_3 = Ga_I–O_2 bending. Only contributions originating from principal force constants greater or equal to 15% are reported. n.o. = not observed.

[c] Numbers correspond to localized coordinates described in Table I and Fig. 3 and which are mainly involved in the LX cartesian displacements.

corresponds to a collective displacement of atoms and is assigned to a translation following the z axis of tetrahedra chains. The 195-cm^{-1} mode represents librations of chains around the y axis. The full description of cartesian displacements can be obtained from the authors.

3. Temperature Effect on the Raman Spectra

The main causes which contribute to the broadening of Raman and infrared lines are the following:

(i) anharmonicity phenomena,

(ii) thermally activated reorientational

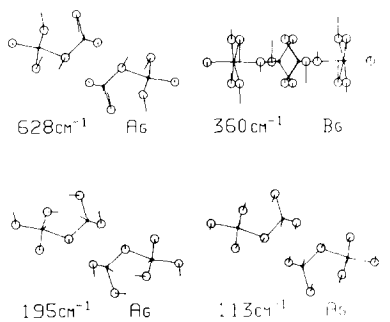

FIG. 8. Relative cartesian displacements of atoms involved in three in-plane (A_g) and one out-of-plane (B_g) normal modes at high and low frequency, respectively. For high-frequency modes oxygen displacements predominate, while at low frequency gallium displacements contribute to a large extent to the normal mode.

processes which, for instance, could involve librations of tetrahedra chains,

(iii) vibrational dephasing (surrounding time fluctuations), and

(iv) creation of defects leading to spectral density, which can be large for dispersive modes.

The reorientational term can be eliminated from the broadening causes; in fact, it usually plays an important role in molecular crystals in which the reorientation of individual groups of atoms or molecules can occur upon increasing the temperature (*11*). This is not the case in a crystal where there exists a tridimensional framework in which the reorientation of tetrahedra chains requires much energy.

(*a*) *Temperature dependence of the half-widths*. The broadening factor of Raman bands in the 10- to 1000-K temperature range is very large. Most of the bands above 300 cm^{-1} broaden by a factor of 15 or 20. On the other hand, the low-frequency modes are much less sensitive to the temperature effect and they broaden only by a factor of 8.

The difference of behavior between high- and low-frequency modes is associated with the difference of the types of motions involved in these modes. Low-frequency modes involve mainly motions of weak amplitude (Fig. 8). On the contrary, high-frequency modes involve motions of large amplitude, mainly for oxygen atoms. However, it is difficult to establish a general rule. In fact, among the low-frequency modes the 147-cm^{-1} band does not follow this behavior; its half-width varies from 2 to 17 cm^{-1}, although it corresponds to a $T'y$ translation of tetrahedra chains with amplitudes very similar to those calculated for the rest of the external modes. Moreover, one can also try to correlate the broadening to the displacement direction of atoms, the B_g mode at 651 cm^{-1} which is assigned to displacements perpendicular to the (010) plane being less broadened than the 360-cm^{-1} mode of B_g symmetry. Therefore it is difficult to establish a correlation without aberrant points. Except for the B_g modes at 147 cm^{-1}, it seems in general that the modes involving oxygen atoms of type II are less broadened than those involving oxygen atoms of type I; in particular, this is the case for the two B_g modes discussed above. In the same way, among the high-frequency modes one can verify that the bands at 763 and 628 and the two modes at 475 cm^{-1} involving the local coordinates 1, 2, 4, and 6, all based on the $Ga_I(O_I)_2$ group of atoms located in the (010) plane, become broader than the 651-cm^{-1} mode, involving the $Ga_I(O_{II})_2$ group of atoms, as if the perturbation acting on the GaO_I vibrators was weaker than that acting on the GaO_{II} ones. These vibrators, being freer from perturbation, could oscillate with a larger amplitude.

(*b*) *Temperature dependence of frequencies*. As an example, we give in Fig. 10 the temperature dependence of frequencies for three modes for which the variations are the largest ones. For comparison we report also two external modes where the frequency variations are much smaller. In the temperature range under study, variations are comparable with those observed for other

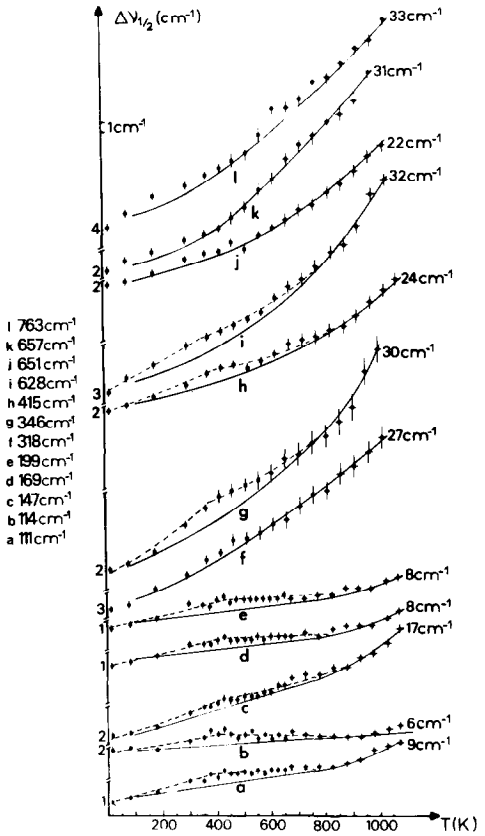

FIG. 9. Experimental Raman band half-widths as a function of temperature. (---) Experimental curve; (——) curve calculated from anharmonic contributions (see text); values of the half-widths are reported on the left and the right parts of the curves for 10 and 1070K, respectively.

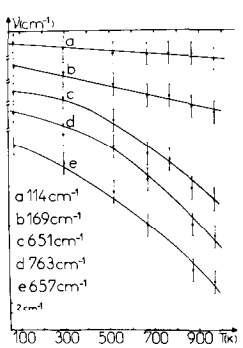

FIG. 10. Raman frequency as a function of temperature (only five representative modes are reported).

crystals. These frequency shifts are connected on the one hand to the volume variation of the material as a function of temperature ($\delta\omega_J$ terms) and on the other hand to the contribution of anharmonicity ($\Delta\omega_J$ terms) (*8*). The terms are connected through the relationship

$$\omega_J(T) = \omega_J(O) + \delta\omega_J + \Delta\omega_J,$$

where $\delta\omega_J$ can be expressed as a function of the Grüneisen coefficient (*9*). Because of the lack of additional data we have not been able to estimate the $\delta\omega_J$ term associated with the volume variation. This will be undertaken in a forthcoming study (*12*).

(*c*) *Broadening of Raman bands due to anharmonicity.* The half-width of bands is usually expressed by the following cubic and quartic terms:

$$\Gamma_{\text{cubic}} = A[(e^{\hbar\omega_0/2kT} - 1)^{-1} + \tfrac{1}{2}], \quad (1)$$

$$\Gamma_{\text{quartic}} = B[(e^{\hbar\omega_0/3kT} - 1)^{-1} + \tfrac{1}{2})^2 + \tfrac{1}{12}], \quad (2)$$

where A and B are two constants.

The cubic term describes the destruction of one phonon of ω_0 frequency into two phonons which can in a first approximation be considered to have a frequency equal to $\omega_0/2$.

In the same way, the quartic term can be associated with the destruction of one phonon of $\omega_0/3$ frequency (*8*). At high temperature, the cubic term is proportional to T and the quartic term to T^2 (*8*, *10*).

We fitted our data with these equations for all the observed modes (except for the mode at 353 cm^{-1} which is smeared out by the 346-cm^{-1} line and for the 475-cm^{-1} band which is a superposition of two modes of A_g and B_g symmetry, respectively); the corresponding A and B parameters are reported in Table V.

The cubic term dominates for the phonon of low frequency, while for high-frequency

TABLE V

CONTRIBUTION OF ANHARMONICITY TO THE RAMAN BANDS HALF-WIDTH (Γ)

Frequency (cm^{-1})	Γ (1000K) (cm^{-1})	A (cm^{-1})	B (cm^{-1})	γ (1000K)	a	b
763	31	7.395	2.006	0.041	9.6	2.6
657	31	3.237	2.204	0.047	4.9	3.4
651	21	1.803	1.497	0.032	2.8	2.3
628	30	4.717	1.604	0.048	7.5	2.6
415	18	1.561	0.439	0.043	3.8	1.1
346	29	1.946	0.554	0.084	5.6	1.6
318	26	3.904	0.193	0.082	12.3	0.6
199	7	0.606	0.011	0.035	3.1	0.06
169	7	0.528	0.008	0.041	3.1	0.05
147	14	0.961	0.017	0.095	6.5	0.1
114	5	0.286	0.	0.044	2.5	0.
111	9	0.364	0.007	0.081	3.3	0.06

Note. A and B are the parameters which are found from the best fit between the experimental curves of Fig. 9 and the expression of $\Gamma_{cubic} + \Gamma_{quartic}$ given in the text. γ, a, b are the Γ, A, B parameters reduced to the frequency of the corresponding mode.

modes, the quartic term can explain by itself the shape of the curves $\Gamma = f(T)$. This can be well understood as far as the probability for the destruction of one phonon at low frequency into three other phonons of $\omega_0/3$ frequency is much lower than for the high-energy phonons (*8*).

(*d*) *Creation of defects upon increasing the temperature.* Most of the curves present an inflection point, and for some of them a horizontal part is even observed (that is the case for the 111-, 114-, 169-, and 199-cm^{-1} modes). The experimental points of Fig. 9 seem to be distributed above the solid-line curve representing the anharmonicity contribution to the half-width. The experimental curves coincide with the calculated curves for temperatures above 700K. This is mainly observed for dispersive modes (external modes) and indicates that an amount of disorder appearing above 100K could be responsible for the breakdown of the $k = 0$ selection rule and this could induce a spectral density. The existence of a horizontal part shows that the rate of disorder seems to be maximum at temperatures as low as 400K. The disorder could originate from the creation of defects (vacancies, occupation of interstitial sites probably by oxygen atoms); in fact, the nonobservation of any peaks in the DTA experiments seems to exclude the possibility of a phase transition of the displacive type (e.g., chain reorientation). Moreover, the large range of temperature in which this broadening is observed indicates that this phenomenon is strongly of second order and should be of the order–disorder type as already observed for some molecular crystals (*11*). Finally, a phase transition could give rise to a frequency discontinuity near the transition temperature and this is not actually observed.

Conclusion

We report a complete assignment of the ir and Raman frequencies of β Ga_2O_3 in terms of symmetry. The spectra are more consistent with the centrosymmetric structure reported by Geller than with that proposed by Wolten.

We propose a description of the normal modes based on:

(i) the potential energy distribution given in terms of internal coordinates,

(ii) the cartesian displacements of the atoms, and

(iii) localized coordinates being chemically significant.

A complete set of force constants is given. The existence of small force constants in the [100] direction is consistent with the observation of a (001) cleavage plane.

The temperature dependence of frequencies and half-widths in the 10- to 1000-K range is mainly due to anharmonicity. The contribution of quartic terms is important for high-frequency modes, while the cubic terms are almost sufficient to explain the broadening of low-frequency lattice modes.

A noticeable increment to the broadening of Raman bands in the 100- to 600-K temperature range is interpreted in terms of a reversible low rate of disorder; defects such as the occupation of interstitial sites, or a slight shift of the stoichiometry, could be put forward.

Acknowledgments

We are thankful to Professor Bougeard for help in the normal coordinate calculations. This work was supported by NATO (No. RG 259.80).

References

1. (*a*) D. DOHY AND G. LUCAZEAU, *J. Mol. Struct.*, in press, XV European Congress of Molecular Spectroscopy, Norwich, 1982; (*b*) D. DOHY, Thèse de 3e cycle, Paris (1982).
2. PH. COLOMBAN AND G. LUCAZEAU, *J. Chem. Phys.* **72,** 1213 (1980), and G. LUCAZEAU, *Solid State Ionics*, in press (1983).
3. S. GELLER, *J. Chem. Phys.* **33,** 676 (1960).
4. G. M. WOLTEN AND A. B. CHASE, *J. Solid State Chem.* **16,** 377 (1976).
5. N. T. MCDEWITT AND W. L. BAUN, *Spectrochim. Acta* **20,** 799 (1964).
6. (*a*) A. REVCOLEVSCHI, unpublished; (*b*) A. REVCOLEVSCHI AND M. DE LA ROCHÈRE, unpublished; (*c*) A. REVCOLEVSCHI AND M. SAURAT, *Rev. Int. Hautes Temp. Refract.* **8,** 291 (1971).
7. T. SHIMANOUCHI, Computer programs for NCT of polyatomic molecules, 1968.
8. T. SAKURAI AND T. SATO, *Phys. Rev. B* **4**(2), 583 (1971).
9. A. K. SOOD, A. K. ARORA, V. UMADEVI, AND G. VENKATARAMAN, *Pramana* **16,** 1 (1981).
10. I. P. IPATOVA, A. A. MARADUDIN, AND R. F. WALLIS, *Phys. Rev.* **155**(3), 882 (1967).
11. K. CHHOR, G. LUCAZEAU, AND C. SOURISSEAU, *J. Raman Spectrosc.* **11**(3), 183 (1981).
12. J. R. GAVARRI, AND D. DOHY, *J. Solid State Chem.*, to be published.